NATURAL SLOPE FAILURES DURING EARTHQUAKES: A CASE STUDY

S.Okusa[I], F.Tatsuoka[II], E.Taniguchi[III] and Y.Ohkochi[IV]

SUMMARY

Several shallow natural slope failures induced by the Izu-Ohshima-Kinkai Earthquake of January 15, 1978 were investigated. The failure surfaces were located between a brittle sandy scoria layer and sensitive soft volcanic ash layer, and in the shallow portion of the soft volcanic ash layer. The shear strength of the soft volcanic ash was measured by in situ cone penetration tests and laboratory shear tests. Since the volcanic ash layer had a high natural water content and a high sensitivity, flow-type slope failures could be triggered by a major shock.The mechanism was well explained by the results of the analyses.

INTRODUCTION

On January 14, 1978, a locally destructive earthquake (M=7.0) whose epicenter was located in Sagami Bay, shook the Izu Peninsula which is situated about 120 km southwest of Tokyo (Fig.1). This earthquake caused considerable damage in the mountainous terrain of the peninsula. The largest aftershock (M=5.8) took place on January 15, with its epicenter below the peninsula. The Izu Peninsula is the southernmost part of the Fossa Magna, which is a large tectonic zone bisecting the main island of Japan.

Natural slopes where large failures occurred in the main shock were located close to the activated faults. Those consisting of pyroclastic

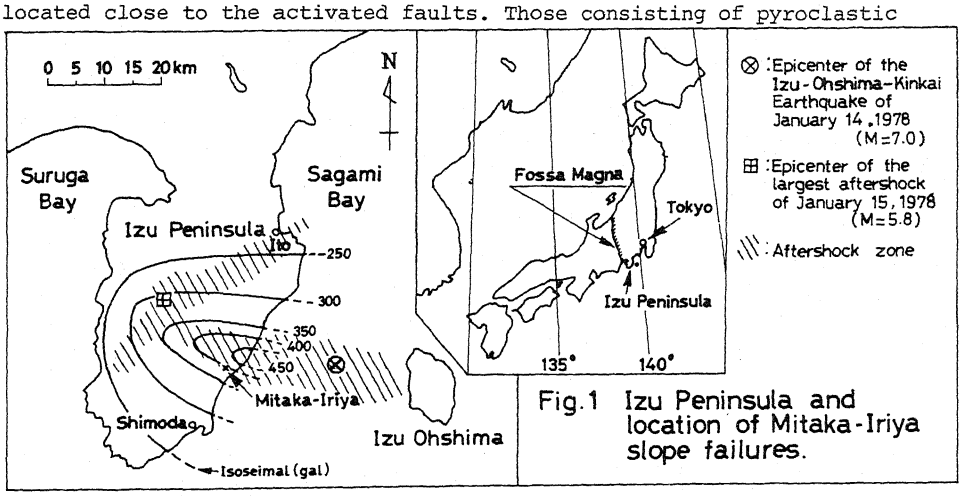

Fig.1 Izu Peninsula and location of Mitaka-Iriya slope failures.

I Professor, Faculty of Marine Science & Technology, Tokai University, Orido 1,000, Shimizu, Shizuoka 424, Japan.

II Associate Professor, Institute of Industrial Science, University of Tokyo, Roppongi 7-22-1, Minatoku, Tokyo 106, Japan.

III Research Engineer, Public Works Research Institute, Ministry of Construction, Toyosatocho, Tsukubagun, Ibaragi 300-26, Japan.

IV Graduate Student, Institute of Industrial Science, University of Tokyo.

material of the late Pleistocene to Holocene were investigated from the viewpoint of soil mechanics.There are several failures of natural slopes located at Mitaka-Iriya, as shown in Fig.2. A cross section typical of the slope failures is illustrated in Fig.3

Slope failure NO.1 is located on recent pyroclastics around 4 km inland from the east coast of the Izu Peninsula. The failed slope had a height difference of 110 m, a maximum width of 200 m, a slope length of 120-200 m and a depth of 2 to 3 m. The slope angle was from 20 to 25° at the upper part and from 25 to 32° at the middle and the lower parts. Around 100,000 m^3 of pyroclastics slid down on a shear plane, like a single plate sliding on a lubricated surface.The vegetation on the top soil also slid down, staying nearly vertical on the sliding soil mass without being seriously damaged. The velocity of the sliding mass was estimated at about 15 m per second or more. This unusually high velocity was estimated from the following observations. Firstly, all seven people (and a dog) who were killed by the landslide were found under the debris near the exits of their houses which were near the toe of the landslide. This indicates that they did not have enough time to escape from the collapsing houses because of the earthquake motion, and that the landslide occurred while they were trying to do so. Furthermore, the sliding mass slid about 30 m up the opposite slope after travelling about 300 m over a small river which ran between the two slopes (as shematically shown in Fig.3). Similar flow-type slope failures took place on slopes NO.2, 3 and 4.

The mountain slopes on the Izu Peninsula with slope angles smaller than around 35° are, in general, covered with aeolian volcanic ashes and scoria of the late Pleistocene to Holocene age. These soft and normally consolidated pyroclastics are from adjacent volcanoes. These formations are believed to be due to a series of periodic volcanic activity. As shown in Fig.3, the most recent volcanic ash is found on the present top surface, with a coarse scoria layer underneath

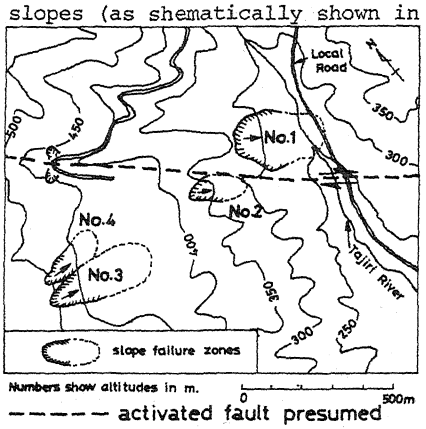

Fig.2 Locations of slope failures at Mitaka-Iriya

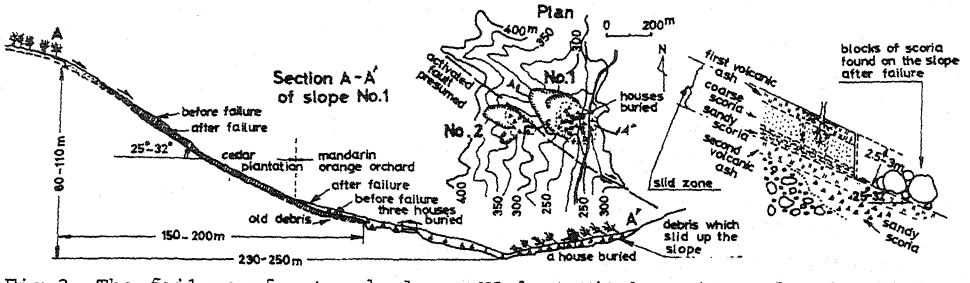

Fig.3 The failure of natural slope NO.1 at Mitaka-Iriya and a detailed cross section (right)

and a sandy scoria layer underneath that. Another older volcanic ash layer was found below the sandy scoria. The older volcanic ash layer will be called the "second ash layer". It seems that after the second volcanic ash layer was formed there was a period with no volcanic activity, resulting in the growth of vegetation on the top surface of that time. Part of the evidence for this deduction is a thin humic layer containing long vertical micropores from the old roots of vegetation, found in the shallow portion of the second volcanic ash layer. The second volcanic ash layer has an extremely high void ratio of around 3 to 4. By examining the the failed slope carefully, it was found that the failure surface was mostly in the shallow portion of the second volcanic ash layer and at the boundary between the second volcanic ash layer and the overlying sandy scoria layer. Slope failure NO.1 was typical of the failures of recent pyroclastic natural slopes during this earthquake.

Many tension cracks were found even in recent pyroclastic slopes around Mitaka-Iriya that had not failed. It was also found that all of the slope failures were close to the activated faults due to this earthquake, and from analysis of damage to various structures, including overturned tombstones, the maximum acceleration was estimated to be around 350 to 450 gals in a horizontal direction (Fig.1).

IN SITU SURVEY

Cone penetration tests, vane tests and undisturbed samplings were performed for the second volcanic ash layer on slopes NO.1 and NO.3 six months after the failure. The locations of cone penetration tests on slope NO.1 are shown in Fig.4. A trench was excavated next to points NO.8 and NO.9 on slope NO.1 as shown in Fig.5. Disturbed samples were taken from the vertical wall of the trench and their natural water content were measured (Fig.6). The grading and the physical properties of volcanic ash from a depth of 0.3 m

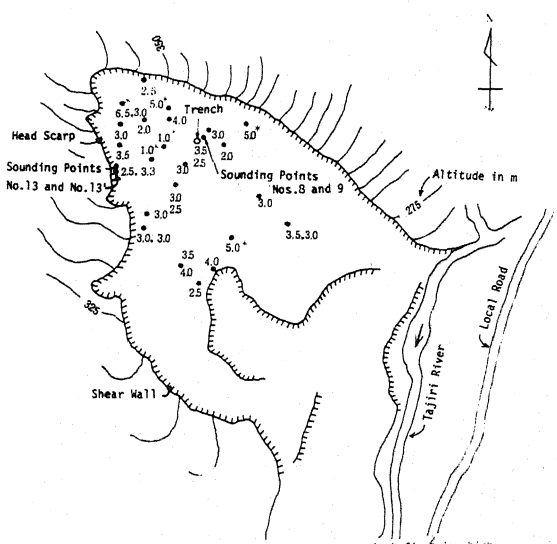

Numbers show the cone penetration resistances q_{c0} in kgf/cm² in which the numbers with * were not used for the analyses.

Fig.4 Cone penetration test network on slope NO.1

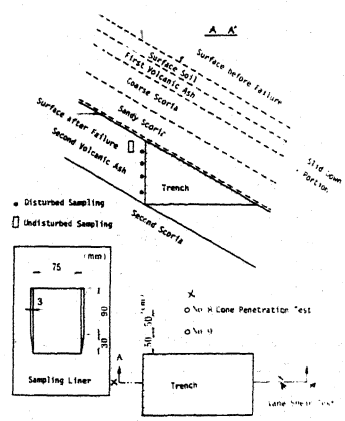

Fig.5 Trench excavated on slope NO.1

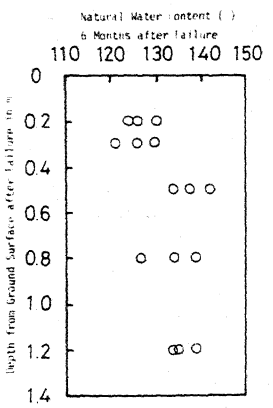

Fig.6 Water content of second volcanic ash layer

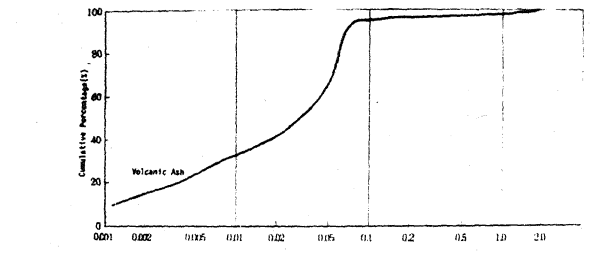

	Unit Weight γ_t (tf/m³)	Void Ratio e	Water Content w_n (%)	Degree of Saturation S_r (%)	Specific Gravity G_s	Liquid Limit w_L (%)	Plastic Limit w_P (%)	Plasticity Index PI (%)
Volcanic Ash	1.26-1.39	2.95-3.90	120.9-129.4	86.4-100.0	2.72-2.75	73.3-97.7	50.8-59.6	22.5-38.2
Scoria	1.31-1.57	1.50-2.17	38.0-46.0	60.2-71.9	2.83-2.85			

Fig.7 Physical properties of volcanic ash and scoria

from the present slope surface are shown in Fig.7. It can be seen from Figs.6 and 7 that the natural water content is around 125% to 135% which is higher than the liquid limit. It should be noted that the volcanic ash is almost saturated. The extremely high water content seems due to the fact that the overlying scoria is permeable and therefore water from rainfall can easily permeate into the volcanic ash layer. The grading curve shown in Fig.7 indicates that the volcanic ash is a mixture of silty and clayey particles.

The cone resistances q_c measured by a double tube cone penetrometer at points NO.8 and NO.9 are shown in Fig.8. The 30° cone with a maximum cross section of 6.46 cm^2 was pushed into the ground at a rate of 1 cm per second. Since the outer tube resisted the friction around the circumference, only the resistances to penetration of the point were measured. A gradual increase in resistance with depth can be seen in Fig.8. The cone resistances q_c at points NO.13 and NO.13' at the head scarp are shown in Fig.9. At these points, some undisturbed scoria was removed to measure cone penetration resistance from the intact surface of the volcanic ash layer to a certain depth. Since almost linear relationships between q_c and depth for shallow portions were obtained, the value of cone penetration resistance at the surface of the volcanic ash layer q_{co} was estimated

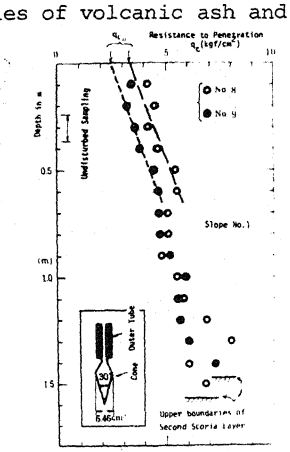

Fig.8 Cone penetration resistance on the middle portion of slope NO.1

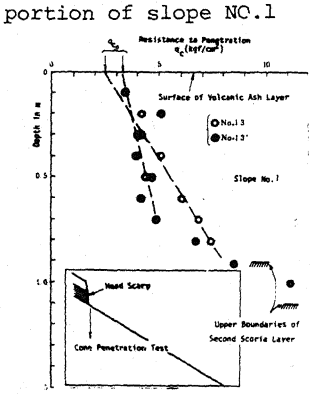

Fig.9 Cone penetration resistance on the head scarp of slope NO.1

by extrapolating the linear relationship to the slope surface as shown in Figs.8 and 9. The values of q_{co} obtained by this procedure are shown in Fig.4. In this figure, the values of q_{co} larger than 5.0 kgf/cm^2 were obtained for the points where the surface that failed was located considerably deeper than the boundary between the sandy scoria and the second ash layer. On the other hand, extremely low q_{co} values of 1.0 kgf/cm^2 were obtained in the gullies which were formed by rainfall after the slope failure. Therefore, it seems reasonable to exclude these high and low values of q_{co} when estimating the value of q_{co} at the moment of failure along the major portion of the failure surface. The average value of q_{co} after excluding extreme values was 3.03 kgf/cm^2 . Since distribution of q_{co} is fairly uniform on the slope surface, the average value of 3.03 kgf/cm^2 was used in the following analyses to estimate the shear strength at the identified failure surface. Similar results for the slope NO.3 are shown in Fig.10.

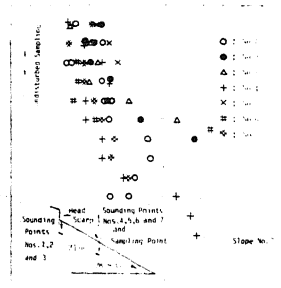

Fig.10 Cone penetration resistance on slope NO.3

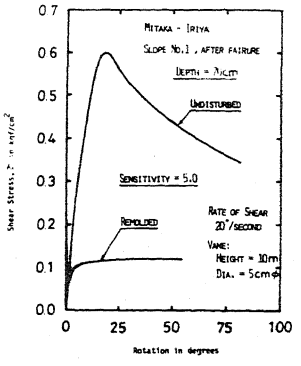

Fig.11 Vane shear strength of second volcanic ash layer on slope NO.1

In situ vane shear tests were performed near the trench on slope NO.1.After rotating the vane rapidly through several rotations, the strength of the remolded soil was also measured. Typical results are shown in Fig.11. The vane shear tests are summarized in Fig.12. It can be seen that the sensitivity is fairly high, ranging from 3.4 to 5.0. Since the sensitivity increases slightly with decreasing depth, it seems reasonable to assume that the sensitivity for the portion shallower than 0.5 m is 4.5 or more. The value of sensitivity obtained by vane shear tests was used in the following analyses.

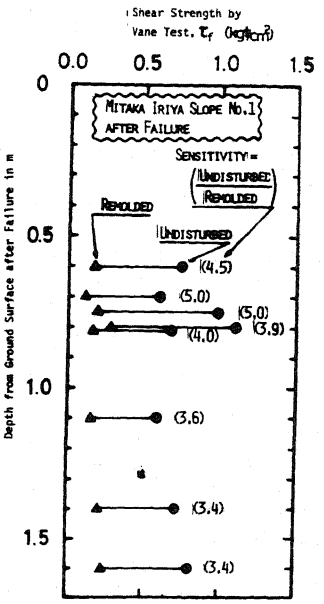

Fig.12 Summary of vane shear tests on slope No.1

LABORATORY SHEAR TESTS

Undisturbed samples were obtained by pushing liners into the second volcanic ash layer to a depth of around 0.3 m. The locations

of sampling were next to the trench on slope NO.1 and at the midpoint of slope NO.3 as shown in Figs.5 and 10, respectively. Unconfined uniaxial tests (U-tests) and consolidated isotropically undrained triaxial compression tests ($\overline{CIU}$-TC tests) were performed to estimate the shear strength along the failure surface. Fig.13 shows a typical result by U-test both for an undisturbed sample and a remolded sample. For slope NO.1, the average value of compressive stress at failure was determined by U-test to be 0.677 kgf/cm^2 . Sensitivity for slope NO.1 is around 5.0 on the average, which is similar to the value obtained by vane shear tests. As indicated in Table 1, the volcanic ash becomes slightly weakened by saturation in $\overline{CIU}$-TU tests. This means that if the second volcanic ash layer was more saturated at the moment of failure than it was at the time of sampling, the shear strength estimated from intact unsaturated samples may be an overestimation. Since it is not possible to estimate the exact moisture condition at the time of failure, the shear strength estimated from intact unsaturated samples was used for the failure envelope of the second volcanic ash layer. It was found in the analyses that the results were not greatly altered when the saturated strength was used. Fig.14 shows the failure envelope used for estimating the shear strength along the failure surface.

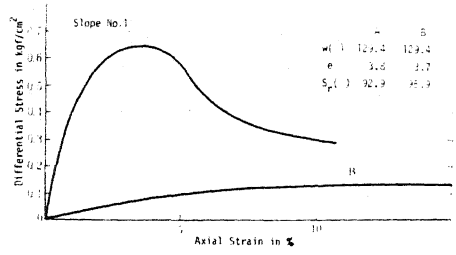

Fig.13 Unconfined strength for undisturbed (A) and remolded (B) samples from second volcanic ash layer

Table 1 Summary of laboratory shear tests

Test Method*	Slope	Sample No.	Void ratio	Water Content( )	Deviatric Stress at Failuere(kgf/cm^2)	Sensitivity
				129.4	0.64	4.9
				125.4	0.64	4.9
				120.9	0.75	5.4
				123.6	0.58	2.9
		1**		124.1	0.85	-
		2**		129.3	0.94	-
		***		125.0	1.22	-

* Samples, 5cm in height and 2cm in diameter in UU test and
5cm in height and 7cm in diameter in CIU-TC test where
back pressure is 2.0kgf/cm^2 for saturated samples with B-values
being larger than 0.9 and effective confining stress is 0.5kgf/cm^2
for all samples.
** Saturated, *** Unsaturated

STABILITY ANALYSES

For safety analyses the shear strength of the failure surface before the failure (S_{uo}) must be determined. Known values are the shear strength for the undisturbed samples from 30 cm depth from the failure surface after the failure (S_{us}) and the cone penetration resistance at the point after the failure (q_{cs}). Assuming that

(1) the value of cone penetration

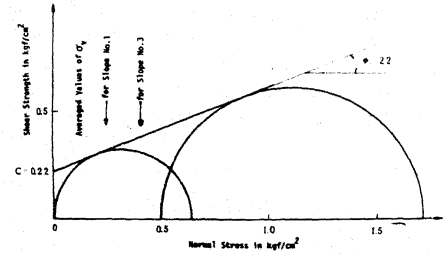

Fig.14 Failure envelope of second volcanic ash layer

resistance q_c is the same before and after the failure,

(2) the shear strength determined for the undisturbed samples taken after the failure S_{us} is the same as in situ shear strength at a sampling depth before the failure and

(3) the rate of increase in q_c in the vertical direction is same as that in the shear strength before the failure,

the shear strength along the estimated failure surface before the failure S_{uo} was calculated as

$$S_{uo} = S_{us} \times q_{co}/q_{cs} \qquad (1)$$

where q_{co} is the cone penetration resistance at the failure surface. The value S_{us} was obtained by reading the value of shear strength corresponding to the overburden stress at the sampling depth before the failure σ_v as shown in Fig.14. The average value of q_{cs} was 4.0 kgf/cm^2 for both slopes NO.1 and NO.3, and the average values of q_{co} were 3.0 kgf/cm^2 for slope NO.1 and 2.5 kgf/cm^2 for slope NO.3. Seismic stabilities of slope NO.1 and slope NO.3 were analyzed by the pseudo-static method illustrated in Fig.15, taking these to be infinite slopes. The factors of safety were calculated as

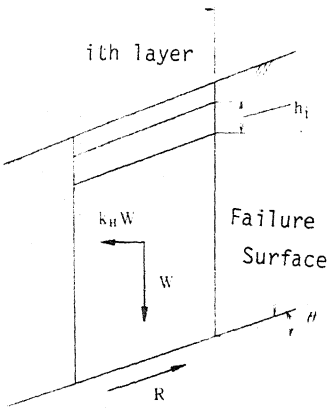

W Selfweight
R Resistance to Shear

Fig.15 Pseudo-static method

$$F_s = \frac{R}{P} = \frac{S_{uo} \cdot \sec\theta}{\sum_i h_i \gamma_i (\sin\theta + k_H \cdot \cos\theta)} \qquad (2)$$

in which θ is the estimated slope angle, h_i and γ_i are the thickness and unit weight of each layer, respectively, and k_H is the horizontal seismic coefficient. Since the observed slope angle ranged from 25° to 32° for slope NO.1 and from 28° to 35° for slope NO.3, the factors of safety for both slopes were calculated using two values of slope angles as function of k_H as shown in Fig.16. It can be seen that F_s becomes less than 1.0 for a k_H larger than about 0.4 for slope NO.1 and around 0.5 for slope NO.3. A k_H of 0.4 corresponds to an acceleration of about 400 gals which is closely comparable with the estimated maximum acceleration at the site, while a k_H of 0.5 seems

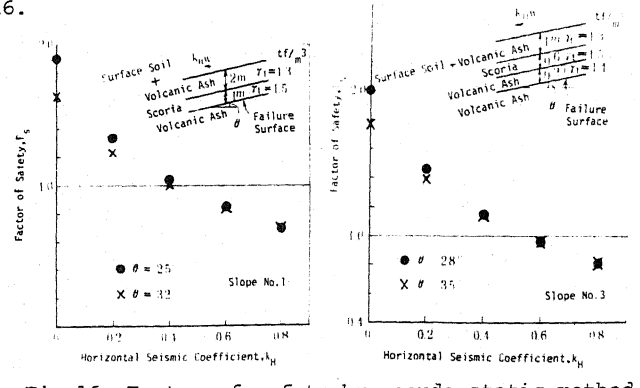

Fig.16 Factor of safety by pseudo-static method

slightly unreasonable.

It seems that the flow-type failure of the slopes at the site is not explained by the results presented above. It should be noted that the value of F_S is considerably larger than 1.0 when k_H=0.0 for both slopes NO.1 and NO.3 and when the shear strength determined from undisturbed samples is used. Contrary to this analytical result, the slides of slopes NO.1 and NO.3 were of the flow-type with a rapid displacement, which can take place only when F_S, without seismic effect, is considerably less than 1.0. This fact suggests that the actual shear strength along the failure surface considerably decreased after the downward displacement was triggered by the major shock of the earthquake. Since the measured sensitivity of the second volcanic ash layer was high (around 5.0 by U-test and about 4.5 or more by vane shear test for slope NO.1), it is likely that the shear strength decreased considerably with the increase in the downward movement. Fig.17 shows the factor of safety when k_H=0.0 for slope NO.1. It was calculated by using shear strength $S_u=S_{uo}/S_t$, in which S_{uo} is obtained by Eq.1 and S_t is the sensitivity. The value of F_S is fairly less than 1.0 for a value of S_t larger than 3.0. To prevent damage due to slope failure, it is not enough simply to know whether displacement is induced; it is also necessary to predict the type of failure. If the displacement ceases after a slight movement, the damage may be unimportant. The damage caused by a slope failure is generally serious if the slope failure is of the flow-type in which the downward displacement is rapid and extremely large.

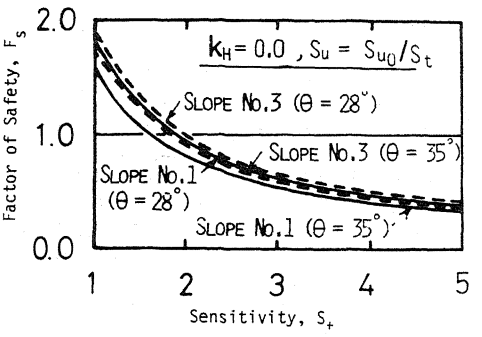

Fig.17 Factor of safety for reduced shear strength

CONCLUSIONS

The investigation of slope failures which occurred during an earthquake showed that to prevent damage it is necessary to predict both the initiation of displacement and the type of failure. The flow-type failure which formed a large, fast-moving mudflow that killed seven people and a dog can be largely attributed to the highly sensitive volcanic ash layer present along the major portion of the failure surface.

ACKNOWLEDGEMENTS

All the authors wish to express their appreciations to Messrs N. Dohi and M. Yoshimura, graduate students of Tokai University, S. Fukushima and H. Igarashi, graduate students of the University of Tokyo, S. Yamada, research technician of the University of Tokyo, H. Ohgaki, undergraduate student of Hosei University, and H. Ogasawara, research assistant in the Ministry of Construction, for their help in performing in situ and laboratory tests.